

Does Leaf Micro-Morphology Influence The Recognition Of Particles On SEM Images?

Samira Muhammad¹, Karen Wuyts¹, Karolien De Wael², Roeland Samson¹

¹Laboratory of Environmental and Urban Ecology, Department of Bioscience Engineering, University of Antwerp, Groenenborgerlaan 171, 2020 Antwerp Belgium

²AXES Research Group, Department of Chemistry, University of Antwerp, Groenenborgerlaan 171, 2020 Antwerp Belgium

Abstract - Scanning electron microscopy (SEM) remains a popular approach to determine the shape, size, density and elemental composition of particles collected on leaf surfaces, but the effect of leaf micro-morphology on particle counts is not very well known. In this study, leaves of sixteen urban plant species were examined for particle density in June and September 2016 using SEM. The investigated plant species differed in leaf micro-morphology involving trichomes, raised stomata, epicuticular wax crystals and convex epidermal cells forming deep grooves between cells. The particle density on leaves of the investigated plant species was estimated by particle size fraction and leaf side. Particle density was significantly higher on the adaxial (AD) leaf side compared to the abaxial (AB) leaf side and higher for fine-particles than coarse-particles. The effect of trichome density on particle density of the AB and the AD leaf side was indicated to be significant and positive for both coarse and fine-particles in June but not in September. The successive repeated measurements elucidated that features constructing the topography of a leaf surface such as trichomes, stomata, and epidermal cells frequently contributed towards the edge enhancement effect, resulting in exaggerated particle counts. Besides, the mechanical drift contributed to the disparity in particle density measurements. Lastly, the reduction in particle density between successive measurements were imputed on the charging effect. These results enable us to suggest that in addition to characterization of micro-morphological features on a leaf surface, SEM will continue to be a useful approach for determining the particle: shape, size, elemental composition and density of the deposited particles. Nonetheless, the disparity in particle density measurements can occur due to abnormal particle recognition. Based on the results of September, we recommend that within-session successive repeated measurements ($\sim n \geq 5$) need to be performed to remove measurement uncertainties and obtain reliable quantitative data of particle counts using SEM

Keywords: Particle recognition, Leaf micro-morphology, Scanning Electron Microscopy (SEM), Edge enhancement, Charging, Drifting

Date Received: 2021-08-16

Date Accepted: 2021-08-26

Date Published: 2021-09-03

© Copyright 2021 Authors - This is an Open Access article published under the Creative Commons Attribution License terms (<http://creativecommons.org/licenses/by/3.0>). Unrestricted use, distribution, and reproduction in any medium are permitted, provided the original work is properly cited.

1. Introduction

Urban plants can reduce atmospheric particulate matter (PM) by capturing them on their leaf surfaces and exposed plant parts [1-5]. However, not all urban plants are equally effective in capturing PM on their leaf surfaces [2-4, 6]. The differences in PM accumulation on leaf surfaces depends on the leaf micro-morphology such as trichomes, epicuticular waxes, and leaf wettability [7-9].

The estimation of PM on leaf surfaces is frequently performed using few specific methods, each with its set of known limitations. The most commonly used techniques is the gravimetric analyses [2-4] where leaf samples are washed using either water, chloroform, or both followed by filtering and weighing. This method provides distribution of surface and in-wax accumulated PM by mass and size fraction. However, Li et al. [10] indicated that water-soluble ions which account for 45 % of the total PM mass in some samples might not be accounted for. Hence, only the water-insoluble PM fraction is quantified, which may increase the likelihood of an under-estimation of the total adsorbed PM. Besides, the dissolved organic particle constituents could be dissolved in chloroform but remain with the removed wax layer after evaporation of chloroform, possibly resulting in higher wax amounts. Another technique for estimating PM collected on leaf surfaces are wind tunnel experiments [11-13]. Overall, wind tunnel experiments may not be a true representation of field conditions [11],

concerning the meteorological and atmospheric conditions and exposure to pollutants. Furthermore, the particles used by the aerosol generator are of a specific diameter and typically single compounds of uniform size [8, 11] which would be an unlikely occurrence in field conditions. Lately, environmental magnetic analyses [14-16] has been frequently used to measure the ferromagnetic and metal component of PM. Saturation Isothermal Remanent Magnetization (SIRM) a proxy for the accumulation of traffic and industry induced particles and has proven to be rapid, affordable and a good indicator for leaf surface accumulated and leaf in-wax immobilized particles [14, 17-20]. The leaf SIRM methodology also has its limitations because it neither quantifies the number of accumulated particles nor does it distinguishes between the size fractions of accumulated particles. However, scanning electron microscopy (SEM) enables the estimation of particle density, its size fraction and elemental composition [21-28]. Besides, SEM is valuable for characterization of leaf: epidermal surfaces, trichomes, and epicuticular wax structures [29-38]. The SEM imaging involves a detection of secondary electrons (SE) which are sample derived-electrons generated from the interaction of the primary electron beam with the top 1-10 nm of the sample surface [39-40] while, the backscattered electrons (BSE) are beam electrons which have been scattered deeper within the sample [41]. The BSE image provides an atomic number map of the investigated specimen [39, 42].

To date, most studies using SEM for examining the particle density did so on leaves of evergreen plant species with sparse to no leaf trichomes [22,25,28], and a rather simple leaf micro-morphology [43] but see the study by Weerakkody et al. [44] on two herbaceous species with hairy leaf surfaces. However, very little is known whether a more complex leaf micro-morphology would allow proper particle density measurements, and whether these results can be replicated. Therefore, the specific objectives of this study were to (a) estimate the density of coarse and fine particles on leaves of perennial deciduous and evergreen plant species ($n = 16$) with complex leaf micro-morphology, and relate it with leaf SIRM of the investigated plant species. The leaf SIRM values have been reported in a separate study by Muhammad et al. [6], (b) identify the effect of leaf micro-morphology, leaf side, exposure time and particle size fraction on particle density and (c) test the repeatability and identify limitations of the methodology by performing time-interval and within-session successive

repeated measurements of particle density on leaves of a subset of plant species ($n = 4$, $n = 5$) respectively. We hypothesize that (i) leaf samples with pronounced leaf micro-morphology, i.e. high trichomes density, convex epidermal cells forming deep grooves between cells, show increased count values in all particle size fractions; (ii) more particles are accumulated on the upward-facing, (i.e., adaxial) leaf side and when leaves are exposed longer; and (iii) repeatability of particle counts is high.

2. Materials and Methods

2.1 Experimental set-up and plant material

The study was conducted as a common-garden experiment on the premises of the University of Antwerp (Antwerp, Belgium). The set-up of the experiment has been fully described by Muhammad et al. [6]. Sixteen plant species including eight deciduous broadleaf tree species: *Catalpa bignonioides*, *Elaeagnus angustifolia*, *Ginkgo biloba*, *Platanus x acerifolia*, *Populus alba*, *Quercus robur*, *Quercus petraea*, *Tilia cordata*, five deciduous broadleaf shrub species: *Buddleja davidii*, *Prunus padus*, *Salix purpurea*, *Sambucus nigra*, *Viburnum lantana*, two evergreen broadleaf species: *Prunus laurocerasus*, *Rhododendron* sp and one climber species: *Hedera helix* were investigated to determine the differences between plant species in the number of leaf-accumulated particles examined by SEM and to characterize the deposited particles by size fraction. The assessment of particle counts using SEM is a resource and time demanding process, hence the number of plant species was limited to 16. This precise set of plant species was selected for the following reasons, (a) leaves of all plant species except *Rhododendron* had pronounced complex leaf micro-morphology, (i.e., sparse to dense trichomes, epicuticular wax crystals, pronounced venation, convex epidermal cells which form deep grooves between cells and raised stomata) and (b) leaves of *Rhododendron* were used as reference plant species as they represent a simple leaf micro-morphology due to the absence of trichomes, epicuticular wax structure of mostly thin film and some platelets, marginally raised stomata and no deep grooves formed between epidermal cells. During the sampling period, the monthly mean minimum and maximum PM_{10} and $PM_{2.5}$ concentrations were 10.7 and 49.9 and 4.4 and 31.7 $\mu g m^{-3}$ respectively. The monthly mean minimum and maximum temperature was 12 and 23 °C respectively. The monthly mean minimum and maximum wind speed were 1 and 6 $m s^{-1}$ respectively. The monthly mean minimum and maximum relative

humidity (RH) was 47 and 92 % respectively. The atmospheric data were obtained from station Antwerpen Luchtbal (42R817) whereas the

meteorological data were obtained from Antwerpen Luchtbal (42M802), operated by Flanders Environment Agency (VMM).

Table 1 The description of leaf micro-morphology for a subset of investigated plant species (n = 16) belonging to respective functional plant types. The text in parenthesis are references of the associated figures (Figure. 1: for deciduous broadleaf trees and Figure. 2: for deciduous broadleaf shrub, evergreen broadleaf shrub and climber species) which illustrate the leaf micro-morphology. The extended dataset for trichome and stomatal density (mm⁻²) has been reported in a study Muhammad et al. [6]. The characterization of epicuticular wax structure (EWS) types has been reported in a study by Muhammad et al [38].

Plant type	Species	Trichomes	Stomata	EWS	Description of leaf micro-morphology
Deciduous broadleaf tree species (Figure 1)	<i>Catalpa bignonioides</i>	Yes (5.29)	422.1	Thin film	Presence of raised stomata and convex epidermal cells form deep grooves between cells.
	<i>Elaeagnus angustifolia</i>	Yes (45.13)	-	Crusts	Presence of marginally raised stomata and epidermal cells forming minor grooves.
	<i>Populus alba</i>	Yes (sparse)	-	Thin film	Presence of partially sunken stomata and prominent epidermal cells.
	<i>Ginkgo biloba</i>	No	56.9	Tubules	Presence of sunken stomata and convex epidermal cells. The adaxial surface shows minor grooves formed between epidermal cells.
	<i>Platanus x acerifolia</i>	Yes (2.08)	-	Platelets	Presence of raised stomata and convex epidermal cells. Deep grooves are formed in between convex epidermal cells on the abaxial leaf side but not on the adaxial leaf side.
	<i>Quercus robur</i>	No	446.7	Platelets	Presence of marginally raised stomata covered with epicuticular wax crystals. The epidermal cells do not form deep grooves between cells.
	<i>Quercus petraea</i>	13.38	551.0	Platelets	Presence of sunken stomata. The epidermal cells do not form deep grooves between cells.
Deciduous broadleaf shrub species (Figure 2)	<i>Tilia cordata</i>	No	-	Platelets	Presence of sunken stomata. The adaxial leaf side shows convex epidermal cells forming deep grooves in between cells.
	<i>Buddleja davidii</i>	Yes (dense)	-	Thin film	The abaxial surface consists of dense network of trichomes (for which density could not be determined) a thin film epicuticular wax layer visible under the trichomes. The adaxial leaf surface shows marginally raised stomata and convex epidermal cells forming grooves in between the cells but no sighting of trichomes.
	<i>Prunus padus</i>	0.13	-	Platelets	The abaxial surface shows epidermal layer divided into multiple papillae with dense wax crystals, trichomes and sunken stomata. The adaxial leaf surface shows convex epidermal cells covered with wax crystals and form deep grooves in between cells.
	<i>Salix purpurea</i>	No	735.9	Platelets	The abaxial surface shows epidermal cells with multiple papillae covered with dense trichomes. The adaxial surface shows epidermal cells forming deep grooves in between and are covered with wax crystals. The stomata appear as sunken on both leaf sides.
	<i>Sambucus nigra</i>	Yes (1.38)	-	Thin film	Presence of trichomes and marginally raised stomata. The adaxial leaf side shows convex epidermal cells forming deep grooves.
Climber (Figure 2)	<i>Viburnum lantana</i>	Yes (8.38)	-	Platelets	Presence of marginally sunken stomata, prominent epidermal cells and stellate trichomes. The adaxial leaf surface shows the epidermal cells forming deep grooves in between cells.
	<i>Hedera helix</i>	Yes (0.58)	-	Platelets	Presence of prominent raised stomata and stellate trichomes. Absence of deep grooves formed between epidermal cells on both leaf sides.
Evergreen broadleaf shrub species (Figure 2)	<i>Prunus laurocerasus</i>	No	179.3	Thin film	Presence of raised stomata and trichomes. The epidermal cells are faintly seen on the abaxial leaf side but appear smooth on the adaxial leaf side
	<i>Rhododendron</i>	No	255.5	Platelets	The appearance of epidermal cells forming subtle grooves between cells and partially raised stomata. No appearance of trichomes on both leaf sides.

2.2. Leaf sampling

Leaf samples were collected twice during the growing season of 2016; first in June (9th and 10th), second in September (1st and 2nd). Only mature, undamaged, and non-infected leaves from all investigated plant species were collected. Leaf samples

from each investigated plant species were collected from the south-east direction of the plant, to eliminate within canopy orientation bias. After harvesting, leaf samples were placed in labelled paper envelopes and transported to the adjacent lab (Laboratory of Environmental and Urban Ecology, University of Antwerp, Belgium) for sample preparation. For particle analyses by SEM only,

one plant replicate per species was utilized to determine the particle counts on both the abaxial (AB) and the adaxial (AD) leaf sides. The identified particles were characterized by their particle size on leaves of investigated plant species. The leaf samples included in this study were the same that were used for leaf SIRM analyses in a separate study by Muhammad et al. [6].

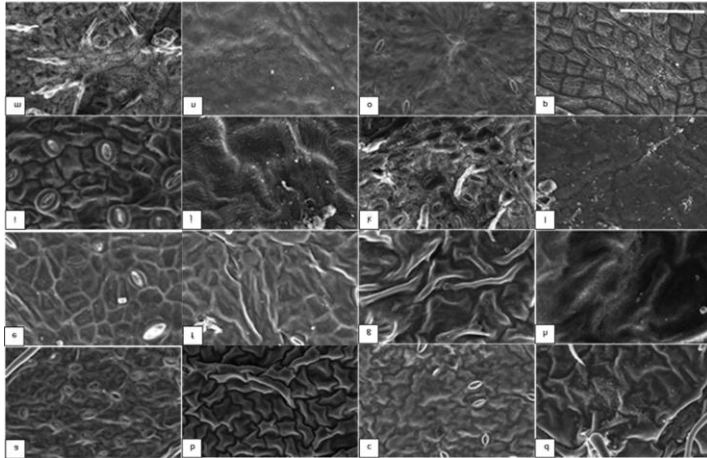


Figure 1 Scanning electron micrographs showing leaf micro-morphology of deciduous broadleaf trees on the abaxial (first and third column) and the adaxial (second and fourth column) leaf sides respectively of (a - b) *C. bignonioides*, (c - d) *E. angustifolia*, (e - f) *P. alba*, (g - h) *G. biloba*, (i - j) *P. acerifolia*, (k - l) *Q. robur*, (m - n) *Q. petraea*, (o - p) *T. cordata*. Scale bar (a - p) = 100 μm .

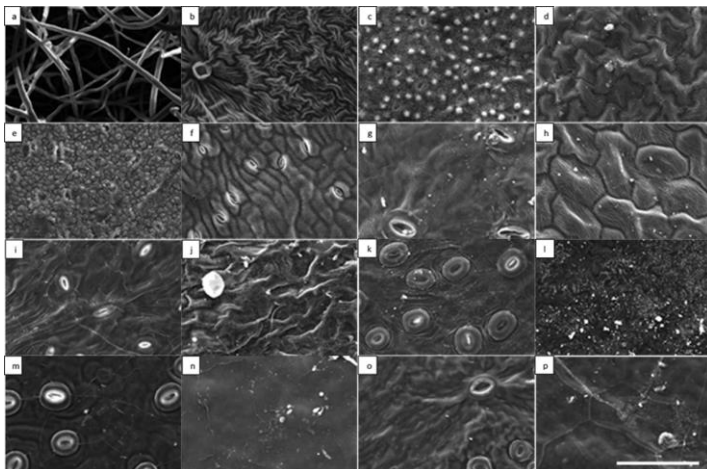


Figure 2 Scanning electron micrographs showing leaf micro-morphology of deciduous and evergreen broadleaf shrub and climber species on the abaxial and the adaxial leaf sides respectively of (a - b) *B. davidii*, (c - d) *P. padus*, (e - f) *S. purpurea*, (g - h) *S. nigra*, (i - j) *V. lantana*, (k - l) *H. helix*, (m - n) *P. laurocerasus*, (o - p) *Rhododendron*. Scale bar (a - p) = 100 μm .

2.3. Sample preparation and scanning electron microscopy (SEM)

The sample preparation was done soon after leaf harvesting using fresh leaf samples. Leaf discs of

approximately 12 mm in diameter were excised using a leaf perforator avoiding the central vein. Leaf discs were placed on an aluminium stub (Ted Pella Inc.) either with the AB or the AD leaf side facing up and affixed in place using conductive double-sided tape (PELCO Tabs 12 mm, 16084-1). The discs were air dried at room conditions. Three days before imaging, the discs were coated with a 20 nm layer of carbon (Leica EM ACE600) in a vacuum environment to avert charge build-up effect. Using a Quanta 250 Field Emission Gun Environmental Scanning Electron Microscope (FEG-ESEM) and the backscattered electron detector, the leaf deposited particles were analyzed within a specified region. The leaf sample surface was subdivided into 100 fields, each field with an area of 209 $\mu\text{m} \times 144 \mu\text{m}$. As such a total surface area of 3.01 mm^2 per sample was considered. The distance between the electron emitter and the sample stage was set to 10 mm. The brightness and contrast settings were set manually based on several particles found on the leaf sample of a specific plant species in order to conceal the leaf micro-morphology in the background while emphasizing only on the particles. This step was performed once before the start of the SEM session for particle count measurements. As such, leaf samples ($n = 4 - 7$) on the sample stage during the session had similar brightness and contrast settings. A spot size of 3.5 with a high vacuum setting of 10^{-3} Pa, incident electron energy of 20 kV and magnification of 1000x was used. The automated software mode (INCA, Oxford Instruments, UK) was used to store features identified as particles on a SEM micrograph with its attributes, (i.e., equivalent circular diameter, length, perimeter, and grey values of the identified particles) in MS Excel format. On a subset of plant species repeated measurements were performed to determine the replicability of particle density in two ways: (i) at relatively large time-interval in different SEM sessions (i.e. months to weeks; $n = 4$) and (ii) at short time-interval within the same SEM session; $n = 5$). For the first, particles were counted on the same samples from the AB and AD leaf side of four species (*G. biloba*, *B. davidii*, *E. angustifolia* and *V. lantana*), on 16th May and 10th, 17th and 31st October, 2017 (T1, T2, T3, T4). For the latter, three successive measurements (M1, M2, M3) of particle counts were performed on each (i.e., AB and AD) leaf side of each of these five plant species within the defined leaf sample region and for the same one hundred fields at each iteration. The within-session successive measurements for a given plant species involving both the AB and the AD leaf sides were performed on the same day. The

particle counts for the 16 investigated plant species for both June and September were examined from March to June 2017 whereas the within-session successive repeated measurements on 5 plant species were performed in May 2018.

2.4. Data analysis

The particles identified on the AB and the AD leaf sides of the investigated plant species ($n = 16$) were classified based on their equivalent circular diameter (ECD) in the following manner; particles $> 10 \mu\text{m}$, $10 \geq$ particle diameter $> 2.5 \mu\text{m}$ (coarse) and $2.5 \geq$ particle diameter $> 0.1 \mu\text{m}$ (fine). The counts of particles with diameter $> 10 \mu\text{m}$ appeared to be negligible compared to the counts in other fractions. Therefore, all statistical analyses were performed on data consisting of particle diameter $\leq 10 \mu\text{m}$. The particle density on leaves of the investigated plant species ($n = 16$) were estimated by dividing the total number of particles in a given size fraction, (i.e., coarse, fine) by the examined leaf area (i.e., 3.01 mm^2) under SEM. Particle density in each size fraction was determined on both the AB and the AD leaf sides. The total particle density per plant species was estimated as the sum of particle density on both the AB and the AD leaf sides consisting of both coarse and fine particles. A linear mixed effects regression (LMER: Bates et al. [45]) was applied on the particle density to examine the effect of particle size fraction (two levels: coarse and fine), time (two levels: June and September), leaf side (two levels: AB and AD) and two-way interaction effects as fixed effects with plant-id as a random effect. The response variable particle density was transformed using the natural log (\ln). A multiple linear regression (MLR) model was applied to determine the effects of leaf traits (trichome and stomatal density, leaf wettability, epicuticular wax structures) on the coarse and fine-particle density on the AB and the AD leaf side in both June and September. Normality of residuals was checked by the Shapiro-Wilk test. The LMER and MLR were initialized using all explanatory variables. Subsequently, model parameters with non-significant ($p > 0.05$) estimates were successively removed. The performances of different LMER and MLR model structures were compared using Akaike Information Criterion (AIC). To identify the relationship between leaf SIRM to particle density, the Pearson correlations were computed individually between natural log-transformed total, coarse and fine-particle density and natural log-transformed leaf SIRM of the investigated plant species ($n = 16$) in both June and September. The coefficient of

variance (CV), calculated as the ratio of standard deviation to the mean and expressed as percentage was calculated on repeated, (i.e., large time-interval different sessions, and within-session successive) measurements of particle density. The effects of leaf traits on the particle density CV (between 0 and 1) were examined using betareg analyses. All statistical analyses were performed using R 3.2.2 software (R core Team 2015), the Stats package (R core Team and contributors worldwide), and the add-on package lmerTest [46]. The XY-plots were generated using the lattice package [47] and stacked bar plots were generated using ggplot2 [48].

3. Results

3.1 Particle density for 16 plant species and its relationship with leaf SIRM

The total particle density (Table 2) in June ranged between 202 and 10981 particles mm^{-2} , with the lowest total density observed on leaves of *S. purpurea* and the highest on leaves of *B. davidii*. The particle densities varied between leaf sides of the investigated plant species in both June and September (Table 2). In June, on the AB leaf side, the coarse-particle density ranged between 3 to 269 particles mm^{-2} and fine-particle density ranged between 42 to 1963 particles mm^{-2} with the lowest density for both particle size fractions were observed on leaves of *T. cordata* and highest on leaves of *V. lantana*. In June, on the AD leaf side, the coarse-particle density ranged between 7 to 709 particles mm^{-2} with the lowest and highest particle density observed on leaves of *Q. robur* and *B. davidii* respectively. The fine-particle density on the AD leaf side ranged between 108 to 9116 particles mm^{-2} with the lowest and highest density observed on leaves of *S. purpurea* and *B. davidii* respectively. In June, the Pearson correlations between natural log-transformed leaf SIRM Muhammad et al. [6] and natural log-transformed total [$r = 0.58$, $df = 14$, $p = 0.02$], coarse [$r = 0.65$, $df = 14$, $p = 0.01$] and fine [$r = 0.58$, $df = 14$, $p = 0.02$] particle density were indicated to be significant and positive (Fig. 3 left). The average \pm SD ratio of fine particle density to the total (fine + coarse) particle density was 0.91 ± 0.02 in June, with lowest fine-particle contributions for *P. alba* (0.87) and highest for *G. biloba* (0.96).

In September, the total particle density ranged between 30 and 1984 particles mm^{-2} with the lowest and the highest total density observed on leaves of *G. biloba* and *P. alba*, respectively (Table 2). In September, on the AB leaf side, the coarse-particle density ranged between 0 to 170 particles mm^{-2} , and the fine-particle density

Table 2 Saturation isothermal remanent magnetization (SIRM: expressed as μA) and particle density (number of particles divided by the area (3.01 mm^{-2}) examined under SEM) of coarse and fine- particles on the abaxial and the adaxial leaf sides of the investigated plant species ($n = 16$) analyzed in June and September 2016. The total particle density is the sum of coarse ($10 - 2.5 \mu\text{m}$) and fine ($2.5 - 0.2 \mu\text{m}$) particle density on the abaxial and the adaxial leaf sides.

Plant Species	June						September					
	SIRM	Abaxial		Adaxial		Total	SIRM	Abaxial		Adaxial		Total
		Coarse	Fine	Coarse	Fine			Coarse	Fine	Coarse	Fine	
<i>Buddleja davidii</i>	6.41	105	1052	709	9116	10981	37.97	15	209	50	528	802
<i>Catalpa bignonioides</i>	3.70	3	68	24	208	303	9.73	10	100	68	514	692
<i>Elaeagnus angustifolia</i>	8.11	134	1797	34	317	2282	14.12	6	29	46	322	402
<i>Ginkgo biloba</i>	3.14	31	205	110	3098	3444	12.89	0	22	0	8	30
<i>Hedera helix</i>	-	7	105	22	248	381	9.09	21	209	54	565	850
<i>Platanus x acerifolia</i>	4.92	8	90	50	467	615	7.01	19	131	17	144	311
<i>Populus alba</i>	2.40	17	155	54	344	571	3.08	170	1620	27	166	1984
<i>Prunus laurocerasus</i>	-	6	76	22	161	265	9.60	2	62	17	251	332
<i>Prunus padus</i>	5.89	7	49	40	464	559	18.15	1	45	17	323	385
<i>Quercus petraea</i>	5.93	4	53	13	155	225	22.10	1	28	50	739	818
<i>Quercus robur</i>	4.26	24	264	7	113	407	21.89	3	98	0	2	103
<i>Rhododendron</i>	-	6	64	42	272	384	15.06	2	56	26	696	780
<i>Salix purpurea</i>	1.34	8	75	12	108	202	8.07	36	390	30	228	683
<i>Sambucus nigra</i>	4.92	30	252	40	383	705	15.58	12	91	44	433	579
<i>Tilia cordata</i>	3.61	3	42	23	250	318	12.76	12	220	25	473	730
<i>Viburnum lantana</i>	15.74	269	1963	401	4632	7265	39.77	26	319	72	698	1116

ranged between 22 to 1620 particles mm^{-2} . The lowest and the highest coarse and fine-particle density was observed on leaves of *G. biloba* and *P. alba* respectively. In September, on the AD leaf side, the coarse-particle density ranged between 0 to 72 particles mm^{-2} , and the fine-particle density ranged between 2 to 739 mm^{-2} . No coarse-particles were detected by SEM on leaves of *Q. robur* and *G. biloba* while the highest coarse-particle density was observed on leaves of *V. lantana*. In September, on the AD leaf side, the lowest and highest fine-particle density was observed on leaves of *Q. robur* and *Q. petraea*, respectively. In September, the Pearson correlation between natural log-transformed leaf SIRM and natural log-transformed total [$r = -0.005$, $df = 14$, $p = 0.98$], coarse [$r = -0.09$, $df = 14$, $p = 0.72$] and fine [$r = 0.004$, $df = 14$, $p = 0.98$] particle density were indicated to be as non-significant (Fig. 3 right). The average \pm SD ratio of fine particle density to the total (fine + coarse) particle density was 0.93 ± 0.03 in September, with lowest fine-particle contributions for *E. angustifolia* (0.87) and highest for *G. biloba* (0.99).

3.2 Particle density: the effect of time, leaf sides and particle size fraction

The results of the LMER model (Table 3) indicated a significant negative effect of time on particle density ($p = 0.004$). The particle density (mean \pm SE) decreased from June (1807 ± 765) to September (662 ± 115). A positive significant effect of leaf side on particle density

was indicated ($p < 0.001$). The particle density on the AD leaf side was 2.6 times higher than the particle density on the AB leaf side. The effect of particle size fraction was indicated to be significant ($p < 0.001$). The coarse-particle density was significantly lower than fine-particle density. The interaction effects between time, leaf sides and particle size fraction on total particle density were indicated to be insignificant.

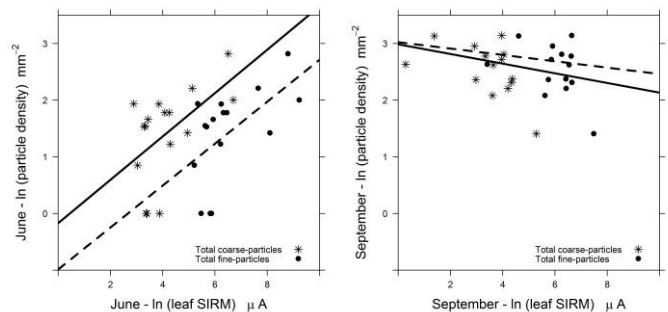


Figure 3 The XY-plot between natural log-transformed leaf SIRM (μA) normalized by leaf area and natural log-transformed total coarse [$\sum(\text{AB coarse-particles, AD coarse-particles})$] and total fine [$\sum(\text{AB fine-particles, AD fine-particles})$] normalized by leaf area examined under SEM (3.01 mm^2) of 16 perennial deciduous and evergreen broadleaf species in June (left) and September (right). The lines represent fitted regression lines; solid for total coarse particles and dashed for total fine-particles

3.3 Effect of leaf traits on particle density

In June, the effect of trichome density was significant and positive on both leaf sides (Fig. 4a, c) and

for coarse and fine particles (Table 3). The fine and coarse-particle density increased with an increase in trichome density. In September, no significant effect of any leaf trait was indicated on either leaf sides (AB and AD) and for both coarse and fine particles (Table 3). However, the XY scatter plot for AD leaf side (Fig. 4d) suggests a weak but positive relationship between trichome and particle density.

Table 3 The multiple linear regression ANOVA of predictor variables (i.e., leaf traits); TR (Trichome density), SD (Stomatal density), EWS (epicuticular wax structures), DCA (drop contact angles) indicating an effect on natural log-transformed ln (particle density) analyzed on the abaxial (AB) and the adaxial (AD) leaf sides for coarse (10 – 2.5 μm) and fine (2.5 – 0.2 μm) particles in June and September. Significant effects ($p \leq 0.05$) are shown in bold

	Fixed factor	F value	p value
Abaxial			
Coarse-particles (June)	TR	5.74	0.031
Fine-particles (June)	TR	7.80	0.014
Coarse-particles (September)	TR	0.06	0.801
	SD	0.26	0.617
	EWS	1.73	0.228
	DCA	0.22	0.650
Fine-particles (September)	TR	0.01	0.939
	SD	0.11	0.746
	EWS	1.66	0.243
	DCA	0.39	0.544
Adaxial			
Coarse-particles (June)	TR	7.54	0.016
Fine-particles (June)	TR	6.62	0.022
Coarse-particles (September)	TR	1.43	0.258
	EWS	2.51	0.117
	DCA	0.22	0.649
Fine-particles (September)	TR	0.72	0.415
	EWS	1.46	0.282
	DCA	0.87	0.371

3.4 Particle counts: repeated measurements on the abaxial and the adaxial leaf sides

The repeated measurements were initially performed on seven samples at large time-intervals in different SEM sessions (data not shown). The coefficient of variance (CV) of these repeated measurements were high and differed between plant species. Additionally, the CV differed between particle size fractions and leaf sides. On the AB leaf side, the CV for coarse and fine-particles ranged between 64 to 112 % and 52 to 91 % respectively. The lowest and the highest CV was observed on leaves of *V. lantana* and *G. biloba* respectively for coarse-particles. The lowest and highest CV for fine-particles was observed on leaves of *E.*

angustifolia and *G. biloba* respectively. On the AD leaf side, the CV ranged between 68 to 137 % and 85 to 108 % for coarse and fine-particles respectively. The lowest and the highest CV for coarse-particles was observed on leaves of *B. davidii* and *G. biloba* respectively. The highest and lowest CV for fine-particles was observed on leaves of *B. davidii* and *V. lantana*. The large time-interval measurements failed to explain the reasons for discrepancies in particle density due to the large CV values, hence within-session successive repeated measurements were performed.

The within-session successive measurements results (Table 4) showed notably smaller CV values. On the AB leaf side the CV ranged between 0 to 50 % and 3 to 37 % for coarse and fine-particles respectively. The lowest and the highest CV for coarse-particles was observed on leaves of *Q. petraea* and *Q. robur* respectively. The lowest and the highest CV for fine particles was observed on leaves of *Q. petraea* and *S. nigra*. On the AD leaf side, the CV ranged between 1 to 25 % and 3 to 20 % for coarse and fine-particles respectively. The lowest and the highest CV was observed on leaves of *Rhododendron* and *S. nigra* respectively for both coarse and fine-particles. Additionally it was observed that the CV increased with an increasing complexity in leaf micro-morphology (*Q. robur* = *S. nigra* > *Q. petraea* = *H. helix* > *Rhododendron*). However, the effect of leaf traits on CV (Table 5) on the AB and the AD leaf side were indicated to be not significant for both the coarse and the fine-particles.

4. Discussion

4.1 Particle density: the differences between plant species and its relationship with leaf SIRM

The investigated plant species showed an effectiveness in collecting particles on their leaf surfaces. The particle densities observed on leaf surfaces of the investigated plant species in this study were notably low when compared with the reported findings of Blanus et al. [13] and Weerakkody et al. [28]. A direct comparison of results from the present study to those of previous studies may be difficult due to the differences in sampling methodologies, sampling locations and investigated plant species. The difference in leaf micro-morphology of the investigated plant species is also another important aspect that could likely cause differences in particle density even within the same genus due to the variation in trichome density, stomatal density, epicuticular wax structure types. Moreover, the differences in particle density of the investigated plant

Table 4 Average particle density and its standard deviation (SD) and coefficient of variation (CV: %) from (within-session) repeated measurements for coarse and fine-particle density on the abaxial (AB) and the adaxial (AD) leaf side of the selected plant species (n = 5) with contrasting leaf micro-morphology. Repeated measurements were performed within a specified region on the leaf sample and one-hundred random fields were examined using SEM. Total - indicates the total particle density (Σ coarse and fine-particles) on both leaf sides. Three consecutive measurements of particle counts are denoted as (M1, M2, and M3). The average, standard deviation (SD) and coefficient variance (CV) expressed as percentage are based on the three repeated measurements of particle density

Plant species	Abaxial (AB)			Adaxial (AD)		
	Coarse	Fine	Total AB	Coarse	Fine	Total AD
<i>Rhododendron</i>						
M1	245	5794	6039	138	915	1053
M2	230	5648	5878	138	933	1071
M3	207	4966	5173	135	873	1008
Average	227	1764	5697	137	907	1044
SD	19	143	460	2	31	32
CV	8	8	8	1	3	3
<i>Hedera helix</i>						
M1	64	804	868	75	1165	1240
M2	60	655	715	73	1091	1164
M3	56	575	630	71	1067	1138
Average	60	678	738	73	1107	1181
SD	4	117	121	2	51	53
CV	7	17	16	3	5	4
<i>Quercus robur</i>						
M1	7	160	167	3	72	75
M2	21	342	363	3	77	80
M3	23	356	379	4	85	90
Average	17	286	303	3	78	82
SD	8	110	118	1	7	7
CV	50	38	39	17	9	9
<i>Quercus petraea</i>						
M1	1	44	45	5	99	104
M2	1	47	48	6	118	125
M3	1	50	51	6	125	131
Average	1	47	48	6	114	120
SD	0	3	3	1	13	14
CV	0	7	6	10	12	12
<i>Sambucus nigra</i>						
M1	306	8508	8814	327	27420	27747
M2	196	5352	5548	212	18819	19031
M3	160	4257	4416	225	20605	20829
Average	220	6039	6259	254	22281	22535
SD	76	2207	2283	63	4539	4602
CV	35	37	36	25	20	20

species could be due to the differences in functional plant types (i.e., deciduous versus evergreen) and the differences in exposure time. Thus a disparity in particle density between the aforementioned studies can be assumed.

In this study, the highest total particle density was observed on leaves of *B. davidii* in June whereas in September the highest total particle density was observed on leaves of *P. alba* (Table 2). The results for *B. davidii* were in agreement with the results reported by Muhammad et al. [6] based on magnetic analyses, however, not in agreement for *P. alba*. Dzierżanowski

and Gawroński [49] found *Populus* species to be highly effective in capturing airborne particles in relation to the ambient air concentrations while Beckett et al. [11] observed a low PM accumulation on leaves of *Populus* species. In the present study, plant species with leaf trichomes, such as *B. davidii*, *E. angustifolia* and *V. lantana* were observed to have a high particle density in June (Table 2). These results were in accordance with the reported findings of previous studies [1-4, 6, 8, 11]. It is possible that trichomes increases the surface area on the leaves where particles can be deposited [50]. Moreover, the boundary layer resistance for leaves with trichomes

is decreased compared to leaves with no trichomes, which makes PM prone to being re-suspended but also enhancing the capture of PM [51].

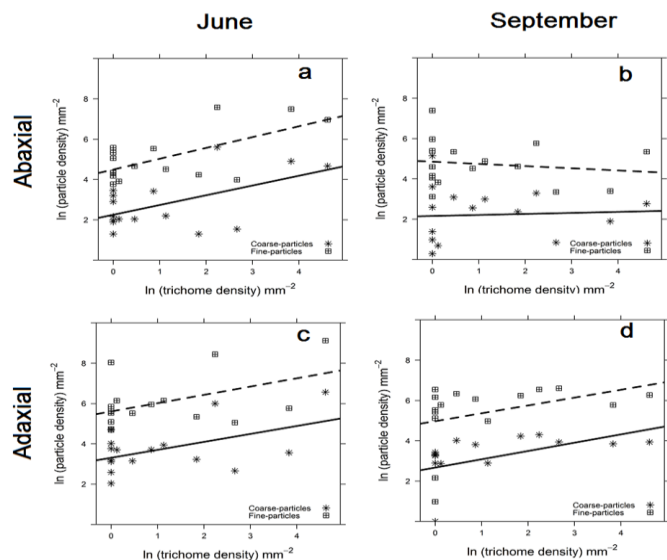


Figure 4 The XY-plot illustrating the relationship between natural log-transformed trichome density and natural log-transformed particle density normalized by leaf area examined under SEM (3.01 mm²) consisting of [coarse (2.5 - 10 μm) and fine (0.2 - 2.5 μm)] particles analyzed in (a) June on the abaxial [AB: coarse ($y = 0.31x + 2.92$, $r = 0.37$), fine ($y = 0.28x + 1.90$, $r = 0.24$)], (c) June on the adaxial [AD: coarse ($y = 0.23x + 2.49$, $r = 0.22$), fine ($y = 0.23x + 3.42$, $r = 0.19$)], (b) September on the abaxial [AB: coarse ($y = 0.19x + 1.74$, $r = 0.02$), fine ($y = -0.14x + 3.11$, $r = 0.02$)], (d) September on the adaxial [AD: coarse ($y = 0.39x + 1.86$, $r = 0.22$), fine ($y = 0.28x + 3.10$, $r = 0.17$)] leaf sides. The lines represent fitted regression lines; solid for coarse-particles and dashed for fine-particles

Table 5 Summary of betareg analyses to determine the effect of leaf traits [stomatal density (SD), drop contact angles (DCA) and trichome density (TR)] on the coefficient of variance (CV) calculated from within-session successive repeated measurements ($n = 3$) for the coarse and the fine-particle density analyzed on the abaxial (AB) and the adaxial (AD) leaf side of 5 perennial deciduous and evergreen plant species

	Effect	Estimate effect size	p value
AB (coarse)	SD	-0.002	0.317
	DCA	0.022	0.117
	TR	-0.114	0.081
AB (fine)	SD	-0.002	0.271
	DCA	0.022	0.114
	TR	-0.101	0.112
AD (coarse)	DCA	0.014	0.436
	TR	0.024	0.717
AD (fine)	DCA	-0.005	0.721
	TR	0.044	0.343

The relationship between particle density (coarse, fine) and leaf SIRM Muhammad et al. [6] of the

investigated plant species was indicated to be significant and positive in June (Fig. 3 left): the higher the density of accumulated particles, the higher the leaf SIRM value. This observation endorses the effectiveness of the SIRM signal of exposed leaves as a proxy for PM exposure. However, no correlation was observed in September (Fig. 3 right). In most studies, refer Hofman et al. [52] for an overview, the relationship with leaf SIRM are established with mass of accumulated particles and atmospheric mass-based PM concentrations, for example, Hofman et al. [20] analyzed the relationship between mass and SIRM of filter membranes and found a significant relationship for large ($\text{PM} > 10 \mu\text{m}$) and coarse (3 - 10 μm) fraction but no significance for fine (0.2 - 3 μm) fraction. This study is, to our knowledge, the first to evidence a relationship between leaf SIRM and the density of leaf-accumulated particles in June. Nonetheless, the absence of an association between particle density and leaf SIRM in September can be ascribed on the limitations of SEM. In practice, the SEM image brightness and contrast settings were adjusted according to the particles found on the leaf sample to highlight only the deposited particles and conceal the leaf micro-morphology in the background. Thus making the detection of particles visibility dependent. It is possible that plant species with leaf trichomes may have some of the deposited particles unaccounted for as they may have been obscured by leaf trichomes. The SEM will emit fewer electrons when particles are obscured by these protuberances, (i.e., trichomes, convex epidermal cells) compared to particles which are situated above these protuberances. In contrast, the SEM may erroneously account these protuberances as particles when their brightness and contrast settings resemble that of a particle. As a result an over estimation of particle density may be encountered as was observed in this study notably for plant species with leaf trichomes. We recognize that the estimation of particle density using SEM accounts for all visible deposited particles, whereas leaf SIRM estimates only the ferro-magnetic and magnetizable component of PM. Nonetheless, the estimation of leaf SIRM is independent of particle visibility, which can be hampered by the deliquescence of hygroscopic particles [53]. Additionally, we were able to distinguish the least and the most effective plant species based on leaf SIRM values Muhammad et al. [6] which were in compliance with the reported findings of previous studies [2-4, 8, 11, 18]. The limitations of SEM are further discussed in detail in § 4.4.

4.2 The effect of time, leaf sides and particle size fractions on particle density

The results of this study indicated a significant decrease in particle density from June to September, which is a rather unexpected outcome. As plant surfaces are in constant contact with their environments they experience repeated episodes of PM exposure, wind and rain resulting in continuous accumulation and removal of particles. Most studies [18, 20, 43, 54] observe a net accumulation of particles with time but an equilibrium of surface particles with those in the surrounding atmosphere has been suggested by Mitchell et al. [1]. Kardel et al. [18] examined leaves of *Tilia* (hairy and non-hairy) and *Carpinus betulus* throughout the growing season, (i.e., May until September) and observed an increase in leaf SIRM towards the end of the growing season. Similarly, Hofman et al. [20] examined the leaf SIRM of *P. x acerifolia* for an entire growing season and observed short-term fluctuations but with a steady increase in leaf SIRM until the onset of leaf senescence. In a separate study, including 96 plant species Muhammad et al. [6] observed an increase in leaf SIRM from June to September and this increase was indicated to be significantly influenced by leaf micro-morphology. In the present work, a decrease in particle density with time was not a plant species-specific observation but an observation for most investigated plant species. A plausible reason for a low particle density in September could be that the same samples were also used for a separate study Muhammad et al. [38] to characterize the epicuticular wax structures types. Due to a considerable reduction in clustering of wax crystals in September, a thorough examination of EW layer was required to determine the EWS type and the extent of loss. In order to secure an area on the sample demonstrating a loss of wax crystals, the examination time was longer than usual. As a result a charging effect was frequently experienced, where a build-up of static electric charges influences the electron signals and deteriorates the image information.

Concerning the differences in particle density on both leaf sides (AB, AD), the particle density was indicated to be more than two times as high on the AD leaf side compared to the AB leaf side as was observed by Ottel  et al. [22]. The higher particle density on the AD leaf side was observed in both June and September and for coarse and fine-particles. It is possible that the AD leaf side due to its orientation in space accumulates more particles through increased sedimentation of particles on the AD side, although a higher resuspension at the AD

side would also be expected as it is more exposed to rain than the AB side. A high particle accumulation typically results in an increased leaf wettability due to hygroscopic effects of the particles [43,55,56]. Litschke and Kuttler [57] suggest that wettable leaf surfaces display an increase in residence time for deposited particles which result in low particle re-suspension rates. An increase in leaf wettability may also increase the foliar uptake of dissolved nitrogen [58-59], dry deposition of water soluble gases such as sulphur dioxide [60], particle accumulation [6, 11, 29, 43, 56, 61, 62] and stimulated growth of phyllosphere microbial communities [63-65]. Concerning the low particle density on the AB leaf side, it was most likely due to the leaf surface roughness caused by the presence of leaf trichomes, stomata and epicuticular wax structures [29] resulting in low leaf wettability. Leaf surfaces demonstrating low wettability are generally anti-adhesive thus facilitating the removal of particles and resulting in clean leaf surfaces [29].

The effect of particle size fraction in this study was indicated to be significant and independent of leaf side and time. The fine-particle density was significantly higher than coarse-particle density. The fine-particle fraction contributed on average by 91 % to the total particle density (fine+coarse). The higher fine-particle density is consistent with the findings of previous studies [22, 28, 66]. In contrast, Dzierzanowski et al. [2] found relatively more coarse than fine-particles on leaf surfaces in terms of mass, using the filter gravimetric method after leaf washing. The disparity in observations can be attributed to the following reasons, (a) the higher mass of coarse-particles compared to fine-particles may result in high weight/area in the gravimetric method, whereas in the SEM image analysis, the number of identified particles of different size fractions are quantified [28] and (b) the proportion of different particle size fraction varies in the atmosphere with different locations. Due to the lack of direct relationship between the number of particles in a given size fraction and their mass, a direct comparison of results may be of little relevance [2]. Grochowicz and Korytkowski [67] elucidated that when fine and ultra-fine particles contribute to 30 % of total PM weight, they comprised of 99.9 % of the total number of particles. The higher incidence of fine particles than coarse particles in terms of counts or density could be as large particles are more easily resuspended in the air compared to small particles [68], hence resulting in low density of coarse particles as observed in this study. Nicholson [69] demonstrated that

the rate of particle resuspension increases with an increase in particle diameter because the drag forces increase quickly compared to adhesive forces [70]. Besides, large particles are protruded further into the turbulent air stream making them prone to resuspension [71].

4.3 The effect of leaf traits on particle density

The effect of leaf wettability, epicuticular wax structures, trichome and stomatal density on the AB and AD particle density were analyzed separately for coarse and fine-particles in both June and September (Table 3). A significant positive effect of trichome density on the AB and the AD particle density was indicated for both coarse and fine particles in June. The fine and coarse-particle density increased with an increase in trichome density (Fig. 4) which corresponds with the findings of studies based on particle mass and on leaf SIRM [1-4, 6, 8, 11, 18, 66]. Plant species with leaf trichomes were observed to immobilize a high (~70 %) fraction of particles on their leaf surfaces compared to plant species with no leaf trichomes (~ 48 %) [72]. Nevertheless, Chen et al. [73] highlighted that the presence of trichomes itself does not ensure an enhanced particle deposition but rather the trichome density is of importance. The presence of trichomes increases the surface area on the leaves where particles can be deposited [50]. Mitchell et al. [1] illustrated that magnetic deposition velocity was higher on leaves with ridged and hairy leaf surfaces. Our study is the first to show that the trichome density influences the number of particles accumulated both in the fine and coarse fraction, ruling out the possibility of trichome density shifting the distribution of accumulated particles towards coarser particles, thereby increasing the accumulation effectiveness of the coarse fraction only and hereby increasing the mass but not the number of particles accumulated. The lack of trichome density effect for both coarse and fine-particles on both AB and AD leaf side in September was rather an unexpected and contrary to the findings in June and the reported findings of past studies [6, 18, 20, 72, 74]. Furthermore, the effect of leaf wettability on particle density was found to be insignificant on both the AB and the AD leaf side, hence the SEM results could not confirm the findings of particle accumulation and immobilization based on magnetic analyses [6, 72].

4.4 Repeatability and limitations of the methodology for particle counts

Despite the significant effect of trichome density on particle density and the significant relationship of particle density with leaf SIRM indicated in June but the lack of (i) relationship between leaf SIRM and coarse and fine-particle density (ii) no significant relationship with leaf traits, and (iii) a decrease in particle density in September made us suspicious towards the September data and solicited for repeated measurements of a subset of plant species. To identify the basis of disparity in particle counts between measurements, the testing conditions in terms of equipment settings (i.e., image brightness, contrast, focus) were set according to the particles found on the leaf sample of a specific plant species prior to the onset of particle count measurements. Initially, the repeated measurements were performed at large time-intervals (data not shown) to determine the cause of discrepancies in particle density. The CV estimated on leaves with trichomes was large and ranged between 52 to 137 % between leaf sides and consisting of both coarse and fine particles. It is worth mentioning that the variation in particle density throughout the repeated measurements was similar for the 5 investigated species, for both leaf sides and both size fractions. This shows that some SEM sessions lead to consistently higher particle density in all samples than other SEM sessions. The large time-interval repeated measurements mostly remained ambiguous and we were unable to identify the exact cause of discrepancies in particle density between measurements. Next, a new subset of plant species was selected possessing simple to complex leaf micro-morphology for within-session successive repeated measurements (Table 4). Moreover, the successive measurements of particle density on the AB and the AD leaf sides of a given plant species were tested on the same day. The within-session successive repeated measurements overall showed CV values ranging between 1 – 50 %. Furthermore, the within-session successive repeated measurements (Table 4) illustrated that as the complexity in leaf micro-morphology increases so did the CV of mean particle density (*Q. robur* = *S. nigra* > *Q. petraea* = *H. helix* > *Rhododendron*). The highest CV was estimated on leaves of *Q. robur* on the AB leaf side and on *S. nigra* on the AD leaf sides. We suppose that leaves of *Q. robur* and *S. nigra* with micro-protuberances in the form of raised stomata, epicuticular wax crystals, dense venation, trichomes and convex epidermal cells (Table 1) possibly resulted in an impediment of accurate particle recognition. Although no significant effect of leaf traits on CV were indicated (Table 5), the SEM images (Fig. 5 a – f) sufficiently

illustrate that leaf micromorphology contributed to the inconsistency in particle density measurements. Postek and Vladár [75] demonstrated that as the beam in a secondary electron image (SEI) approaches an edge of a surface (i.e., trichomes, raised stomata) it generates more secondary electron signal resulting in enhancement of the topographical features (Fig. 5 a – f). To verify the enhancement effects, we compared the SEI and BSE images of *S. nigra* simultaneously. It was observed that enhancement effect was not limited to only the micro-morphological features of the leaf surface (Fig. 5) but also occurred in situations when biological material such as insects were found on the leaf sample (Fig. 5 a, b). Hence, we conclude that measurements of particle density using SEM are complicated by the presence of trichomes, raised stomata and/or convex epidermal cells contributing to the edge enhancement effects.

In addition, through a detailed examination of BSE images of *S. nigra*, it was revealed that the leaf sample of *S. nigra* encountered a mechanical drift during successive measurements. The drift in Figure 5 may not be obvious initially but a more thorough observation reveals that the particle highlighted in green in (Fig. 5g) appears in the top right corner whereas in (Fig. 5h) it appears even further in the top right corner. Moreover, two more particles appear in (Fig. 5h) on the lower left side which were absent in (Fig. 5g). A mechanical drift typically occurs because the column of SEM is directly coupled to the sample stage and any external vibrations transmitted through the frame and isolation system to the column can be transferred to the sample resulting in undesirable artefacts [76]. Other factors which may cause a mechanical drift include any movements in sample stage and friction in its components, changes in atmospheric pressure, small temperature changes in the lens cooling system, or electromagnetic interference [76]. Due to the automated and time-consuming process of particle counts, the samples of plant species ($n = 5$) used for repeated measurements (Table 4) were routinely left unattended. Hence, we remain oblivious to the exact cause of mechanical drift. The findings of our study may not be of fundamental importance when identifying and characterizing the shapes of the micro-morphological features occurring on leaf surfaces (e.g., trichomes, epicuticular wax structures). However, for nano-scale quantitative particle measurements, any distortion may result in erroneous and less reliable data [76].

The within-session repeated measurements, in general displayed a reduction in particle density (coarse and fine-particles) at each subsequent iteration (Table 4) on both the AB and the AD leaf side. We suppose that the reduction in PM density at each iteration was due to the charging effect on the leaf sample. The build-up of voltage on the leaf sample may cause significant variation in the number of secondary electrons detected, resulting in charging artefacts [77-79]. Previous studies [80-83] have studied the charging effects on samples analyzed using SEM. It has been repeatedly stated that when electrons come in contact with the leaf sample they are trapped within the leaf sample due to their non-conductive nature, a negative electrical potential builds up resulting in a brighter image [83]. However, when more electrons are emitted from the leaf sample compared to the primary electron beam, the image appears to be darker [83]. Furthermore, particles which are marginally adhered to the leaf surface tend to blast-off and disappear permanently upon negative charging [83]. It is possible to decrease this charging effect by coating the leaf samples with a thin layer of conducting material, although it does not seem to be possible to achieve a completely conductive coating [84].

Scanning electron microscopes with their tremendous advancements and superior performance [75] have become a favourable tool within the biological and ecological scientific community. Plenty of previous studies [21-23, 25-28] have successfully analyzed elemental composition of the identified particles by employing energy-dispersive X-ray (EDX) spectroscopy. Hence, producing high-quality elemental distribution maps of composite samples [84]. Moreover, a surge in the use of SEM for characterization of epidermal surfaces, trichomes, and epicuticular wax structures [29-38] has been exemplary. Based on (i) the order of magnitude of the particle density data for June, (ii) the significant positive effect of trichome density on particle density for both coarse and fine-particles and (iii) the significant positive relationship with leaf SIRM, we believe that SEM will continue to be a useful methodology for analyzing particle density in addition to the particle shape, size and elemental composition. However, like any other scientific instrument, SEM has its limitations for particle counting, as observed in our study due to edge enhancement, charging effects and mechanical drift. Furthermore, Burkhardt [53] stresses that particles those arrive at leaf surface in liquid phase, remain amorphous rather than becoming crystalline, this makes them difficult to see by SEM resulting in an

underestimation of particles. These shortcomings should not be overlooked. We remain convinced that leaf samples from September endured excessive charging effect leading to contradictory and inconclusive results. In order to obtain reliable quantitative data for particle density using SEM, the within-session successive repeated measurements ($\sim n \geq 5$) need to be a preferred practice.

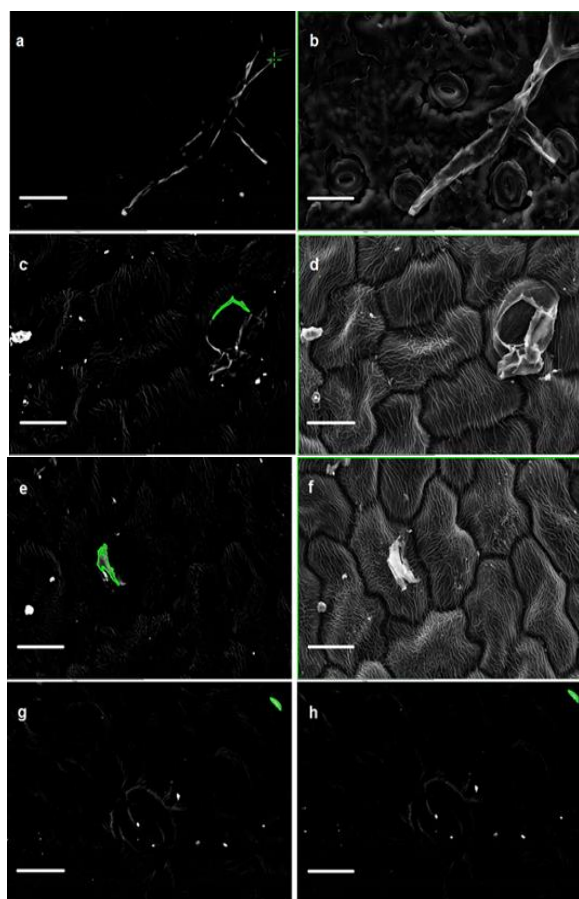


Figure 5 A comparison of backscattered electron image (a, c, e, g-h) with secondary electron image (b, d, f) illustrating the edge enhancement effect (a – f) on leaves of *H. helix* (a and b) and *S. nigra* (c to f). Drifting of leaf sample illustrated on leaves of *S. nigra* (g and h) although subtle, the particle highlighted in green in Fig. 5g appears in the top right corner whereas in Fig. 5h it appears further in the top right corner. Moreover, two more particles appear in Fig. 5h on the lower left side which were absent in Fig. 5g. Scale bar (a- h = 100 μ m).

5. Conclusion

The accumulated-particle density differed between plant species. More particles accumulate on the AD leaf side than on the AB leaf side and density was higher for fine-particles than for coarse-particles. The particle density was influenced by leaf traits, as the

particle density increased with an increase in trichome density in June. In addition, the particle density related significantly with the leaf SIRM in June, confirming the effectiveness of the leaf SIRM as PM exposure proxy. Based on the findings of September, with lower particle density compared to June and no relationship with either leaf trait or with the leaf SIRM, this made us question the reliability of the methodology for particle counting. Our study provides insights on how the complexity of leaf micro-morphology may hinder in particle recognition and accuracy of particle density estimated on leaf surfaces using SEM. The successive repeated measurements enabled us to identify three commonly occurring perils of SEM when estimating particle counts on leaf surfaces with complex micro-morphology. First, the edge enhancement effect was frequently observed on leaves with pronounced micro-morphology consisting of features such as trichomes, raised stomata or convex epidermal cells which construct the topography of the leaf surface. The electron beam generates more secondary electron signal as it scans through those topographical features resulting in the edge enhancement effect followed by measurement errors. Second, it was identified that a mechanical drift was another likely cause that contributed in disparity of particle density. Third, we impute a reduction in particle density between successive measurements on charging effects of the leaf sample due its non-conductive nature. Considering those particles which are loosely adhered to the leaf surface, a negative charging may blast-off those particles permanently causing a reduction in particle density. Based on the findings of June, we believe that SEM will continue to be a useful methodology for analyzing particle density. Based on the results of September, we recommend that within-session successive repeated measurements ($\sim n \geq 5$) need to be performed to remove measurement uncertainties and obtain reliable quantitative data using SEM.

References

- [1] Mitchell, R., Maher, B.A., Kinnersley, R., 2010. Rates of particulate pollution deposition onto leaf surfaces: Temporal and interspecies magnetic analyses. *Environmental Pollution* 158: 1472 - 1478.
- [2] Dzierzanowski, K., Popek, R., Gawronska, H., Sæbø, A., Gawronski, S.W., 2011. Accumulation of particulate matter by several plant species in regard to PM fractions and deposition on leaf surface and in waxes. *International Journal of Phytoremediation* 13: 1037 - 46.

- [3] Sæbø, A. Popek, R., Nawrot, B., Hanslin, H.M., Gawrońska, H., Gawroński, S.W., 2012. Plant species differences in particulate matter accumulation on leaf surfaces. *Science of Total Environment* 427- 428: 347 - 354.
- [4] Popek, R., Gawrońska, H., Wrochna, M., Gawroński, S.W., Sæbø, A., 2013. Particulate matter on foliage of 13 woody species: Deposition on surfaces and phytostabilisation in waxes - a 3-year study. *International Journal of Phytoremediation* 15: 245 - 256.
- [5] Przybysz, A., Sæbø, A., Hanslin, H.M., Gawroński, S.W., 2014. Accumulation of particulate matter and trace elements on vegetation as affected by pollution level, rainfall and the passage of time. *Science of Total Environment* 481: 360 - 69.
- [6] Muhammad, S., Wuyts, K., Samson, R., 2019. Atmospheric net particle accumulation on 96 plant species with contrasting morphological and anatomical leaf characteristics in a common garden experiment. *Atmospheric Environment* 202: 328 - 344.
- [7] Jouraeva, V.A., Johnson, D.L., Hassett, J.P., Nowak, D.J., 2002. Differences in accumulation of PAHs and metals on the leaves of *Tilia x euchlora* and *Pyrus calleryana*. *Environmental Pollution* 120: 331 - 338.
- [8] Freer-Smith, P.H., El-Khatib, A.A., Taylor, G., 2004. Capture of Particulate Pollution by Trees: A Comparison of Species Typical of Semi-Arid Areas (*Ficus Nitida* and *Eucalyptus Globulus*) with European and North American Species. *Water Air and Soil pollution*. 155: 173 - 187.
- [9] Terzaghi, E., Wild, W., Zacchello, G., Cerabolini, B.E.L., Jones, K.C., Di Guardo, A., 2013. Forest filter effect: Role of leaves in capturing / releasing air particulate matter and its associated PAHs. *Atmospheric Environment* 74: 378 - 384.
- [10] Li, X., Wang, L., Wang, Y., Wen, T., Yang, Y., Zhao, Y., Wang, Y., 2012. Chemical composition and size distribution of airborne particulate matters in Beijing during the 2008 Olympics. *Atmospheric Environment* 50: 278 - 286.
- [11] Beckett, K.P., Freer-Smith, P., Taylor, G., 2000. Effective tree species for local air quality management. *Journal of Arboriculture*. 26: 12 - 19.
- [12] Räsänen, Janne V., Holopainen, T., Joutsensaari, J., Ndam, C., Pasanen, P., Rinnan, Å., Kivimäenpää, M., 2013. Effects of species-specific leaf characteristics and reduced water availability on fine particle capture efficiency of trees. *Environmental Pollution* 183: 64 - 70.
- [13] Blanus, T., Fantozzi, F., Monaci, F., Bargagli, R., 2015. Leaf trapping and retention of particles by holm oak and other common tree species in Mediterranean urban environments. *Urban Forestry and Urban Greening* 14: 1095 - 1101.
- [14] Matzka, J., Maher, B. A., 1999. Magnetic biomonitoring of roadside tree leaves: Identification of spatial and temporal variations in vehicle derived particles. *Atmospheric Environment*. 33: 4565 - 4569.
- [15] Muxworthy, A. R., Matzka, J., Petersen, N., 2001. Comparison of magnetic parameters of urban atmospheric particulate matter with pollution and meteorological data. *Atmospheric Environment*. 35: 4379 - 4386.
- [16] Jordanova, D., Petrov, P., Hoffmann, V., Gocht, T., Panaiotu, C., Tsacheva, T., Jordanova, N., 2010. Magnetic signature of different vegetation species in polluted environment. *Studia Geophysica et Geodaetica* 54: 417 - 442.
- [17] Ubat, M., Lehdnroff, E., Schwark, I., 2004. Biomonitoring of air quality in the Cologne conurbation using pine needles as a passive sampler-part I: magnetic properties. *Atmospheric Environment* 38: 3781-3792.
- [18] Kardel, F., Wuyts, K., Maher, B.A., Hansard, R., Samson, R., 2011. Leaf saturation isothermal remanent magnetization (SIRM) as a proxy for particulate matter monitoring: Inter-species differences and in season variation. *Atmospheric Environment*. 45: 5164 - 5171.
- [19] Sant'Ovaia, H., Lacerda, M.J., Gomes, C., 2012. Particle pollution - An environmental magnetism study using biocollectors located in northern Portugal. *Atmospheric Environment* 61: 340 - 349.
- [20] Hofman, J., Wuyts, K., Van Wittenberghe, S., Brackx, M., Samson, R., 2014. On the link between biomagnetic monitoring and leaf-deposited dust load of urban trees: Relationships and spatial variability of different particle size fractions. *Environmental Pollution* 189: 63 - 72.
- [21] Tomašević, M., Vukmirović, Z., Rajšić, S., Tasić, M., Stevanović, B., 2005. Characterization of trace metals particles deposited on some deciduous tree leaves in an urban area. *Chemosphere* 61: 753 - 760.
- [22] Ottelé, M., van Bohemen, H.D., Fraaij, A.L.A., 2010. Quantifying the deposition of particulate matter on climber vegetation on living walls. *Ecological Engineering* 36: 154 - 162.
- [23] Pourkhabbaz, A., Rastin, N., Olbrich, A., Langenfeld-Heysler, R., Polle, A., 2010. *Bulletin of Environmental Contamination and Toxicology* 85: 251 - 255.
- [24] Weber, F., Kowarik, I., Saumel, I., 2014. Herbaceous plants as filters: Immobilization of particulates along urban street corridors. *Environmental Pollution* 186: 234 - 240.
- [25] Song, Y., Maher, B.A., Li, F., Wang, X., Sun, X., Zhang, H. 2015. Particulate matter deposited on leaf of five evergreen species in Beijing, China: Source identification and size distribution. *Atmospheric Environment* 105: 53 - 60.
- [26] Castanheiro, A., Samson, R., De Wael, K., 2016. Magnetic-and particle-based techniques to investigate metal deposition on urban green. *Science of The Total Environment* 571: 594 - 602.
- [27] Sgrigna, G., Baldacchini, C., Esposito, R., Calandrelli, R., Tiwary, A., Calfapietra, C., 2016. Characterization of leaf-level particulate matter for an industrial city using electron microscopy and X-ray microanalysis. *Science of the Total Environment* 548 - 549: 91 - 99.
- [28] Weerakkody, U., Dover, J. W., Mitchell, P., Reiling, K., 2017. Particulate matter pollution capture by leaves of seventeen living wall species with special reference to rail-traffic at a metropolitan station. *Urban Forestry and Urban Greening* 27: 173 - 186.

- [29] Neinhuis, C., Barthlott, W., 1997. Characterization and distribution of water-repellent, self-cleaning plant surfaces. *Annals of Botany* 79:667 - 677.
- [30] Barthlott, W., Neinhuis, C., Cutler, D., Ditsch, F., Meusel, I., Theisen, I., Wilhelmi, H., 1998. Classification and terminology of plant epicuticular waxes. *Botanical Journal of the Linnean Society* 126: 237 - 260.
- [31] Wagner, P., Fürstner, R., Barthlott, W., Neinhuis, C., 2003. Quantitative assessment to the structural basis of water repellency in natural and technical surfaces. *Journal of Experimental Botany* 54: 1295 - 1303.
- [32] Shepherd, T., Griffiths, D.W., 2006. The effects of stress on plant cuticular waxes. *New Phytologist* 171:469-499.
- [33] Bhushan, B., Jung, Y.C., 2008. Wetting, adhesion and friction of superhydrophobic and hydrophylic leaves and fabricated micro/nanopatterned surfaces. *Journal of Physics: Condensed Matter* 20: 225010.
- [34] Koch, k., Ensikat, H.J., 2008. The hydrophobic coatings of plant surfaces: Epicuticular wax crystals and their morphologies, crystallinity and molecular self-assembly. *Micron* 39: 759 - 772.
- [35] Koch, K., Barthlott, W., 2009. Superhydrophobic and superhydrophylic plant surfaces: an inspiration for biomimetic materials. *Philosophical Transaction of the Royal Society A* 367:1487-1509.
- [36] Koch, K., Bhushan, B., Barthlott, W., 2009. Multifunctional surface structures of plants: An inspiration for biomimetics. *Progress in Materials Science* 54: 137 - 178.
- [37] Burkhardt, J., Pariyar, S., 2014. Particulate pollutants are capable to degrade epicuticular waxes and to decrease drought tolerance of Scots pine (*Pinus sylvestris* L.). *Environmental Pollution* 184: 659 - 667.
- [38] Muhammad. S., Wuyts, K., Nuyts, G., De Wael, K., Samson, R. 2020. Characterization of epicuticular wax structures on leaves of urban plant species and its association with leaf wettability. *Urban Forestry and Urban Greening* 47: 126557.
- [39] Goldstein, J., Newbury, D., Joy, D., Lyman, C., Echlin, P., Lifshin, E., Sawyer, L., Michael, J., Scanning electron microscopy and X-Ray microanalysis 3rd Ed. USA: Springer 2003.
- [40] Stokes, D.J., Principles and practice of variable pressure/environmental scanning electron microscopy (VP-SEM). UK: John Wiley and Sons Ltd; 2008.
- [41] Talbot, M.J., White, R.G., 2013. Cell surface and cell outline imaging in plant tissues using backscattered electron detector in a variable pressure scanning electron microscope. *Plant Methods* 9: 40.
- [42] Winter, N., Scanning Electron Microscopy of Cement and Concrete. 2012. WHD Microanalysis Consultants Ltd. pages 1 - 20.
- [43] Neinhuis, C., Barthlott, W., 1998. Seasonal changes of leaf surface contamination in beech, oak, and ginkgo in relation to leaf micromorphology and wettability. *New Phytologist* 138: 91 - 98.
- [44] Weerakkody, U., Dover, J. W., Mitchell, P., Reiling, K., 2018. Evaluating the impact of individual leaf traits on atmospheric particulate matter accumulation using natural and synthetic leaves. *Urban Forestry and Urban Greening* 30: 98 - 107.
- [45] Bates, D., Mächler, M., Bolker, B., & Walker, S. (2015). Fitting Linear Mixed-Effects Models Using lme4. *Journal of Statistical Software* 67(1): 1 - 48.
- [46] Kuznetsova, A., Brockhoff, P.B., Christensen, R.H.B., 2017. lmerTest Package: Tests in Linear Mixed Effects Models. *Journal of Statistical Software* 82: 1 - 26.
- [47] Deepayan, S., 2008. Lattice: Multivariate Data Visualization with R. Springer, New York. ISBN 978-0-387-75968-5.
- [48] Wickham, H., 2009. ggplot2: Elegant Graphics for Data Analysis. Springer-Verlag New York.
- [49] Dzierzanowski, K., Gawronski, S.W., 2011. Use of trees for reducing particulate matter pollution in air. *Challenges of Modern Technology* 12: 69 - 73.
- [50] De Nicola, F., Maisto, G., Prati, M.V., Alfani, A., 2008. Leaf accumulation of trace elements and polycyclic hydrocarbons (PAHs) in *Quercus ilex* L. *Environmental Pollution* 153: 376 - 83.
- [51] Bakker, M.I., Vorenhout, M., Sijm, D.T.H.M., Kollöffel, C., 1999. Dry deposition of atmospheric polycyclic aromatic hydrocarbons in three *Plantago* species. *Environmental Toxicology and Chemistry* 18: 2289 - 94.
- [52] Hofman, J., Maher, B.A., Muxworthy, A.R., Wuyts, K., Castanheiro, A., Samson, R., 2017. Biomagnetic monitoring of atmospheric pollution: a review of magnetic signatures from biological sensors. *Environmental Science and Technology* 51(12):6648-6664.
- [53] Burkhardt, J., 2010. Hygroscopic particles on leaves: nutrients or desiccants? *Ecological Monographs Ecological Society of America* 80(3):369-399.
- [54] Lehdnroff, E., Urbat, M., Schwark, L., 2006. Accumulation histories of magnetic particles on pine needles as function of air quality. *Atmospheric Environment* 40(36): 7082 - 96.
- [55] Crosseley, A., Fowler, D., 1986. The weathering of Scots pine epicuticular wax in polluted and clean air. *New Phytologist* 103:207-218.
- [56] Cape, J.N., Paterson, I.S., Wolfenden, J., 1989. Regional variation in surface properties of Norway spruce and Scots pine needles in relation to forest decline. *Environmental Pollution* 58: 325 - 342.
- [57] Litschke, T., Kuttler, W., 2008. On the reduction of urban particle concentration by vegetation - a review. *Meteorologische Zeitschrift* 17: 229 - 240.
- [58] Adriaenssens, S., Staelens, J., Wuyts, K., De Schrijver, A., Van Wittenberghe, S., Wuytack, T., Kardel, F., Verheyen, K., Samson, R., Boeckx, P., 2011. Foliar nitrogen uptake from wet deposition and the relation with leaf wettability and water storage capacity. *Water Air Soil Pollution* 219: 43 - 57.
- [59] Wuyts, K., Adriaenssens, S., Staelens, J., Wuytack, T., Wittenberghe, S.V., Boeckx, P., Samson, R. Verheyen, K., 2015. Contributing factors in foliar uptake of dissolved inorganic nitrogen at leaf level. *Science of the Total Environment* 505: 992-1002.

- [60] Zhang, L., Brook, J.R., Vet, R., 2003. A revised parameterization for gaseous dry deposition in air-quality models. *Atmospheric Chemistry and Physics. European. Geosciences Union* 3: 2067 – 2082.
- [61] Cape, J.N., 1983. Contact angles of water droplets on needles of Scots pine (*Pinus sylvestris*) growing in polluted atmospheres. *New Phytologist* 93:293-299.
- [62] Beckett, K.P., Freer-Smith, P. H., Taylor, G., 1998. Urban woodlands: their role in reducing the effects of particulate pollution. *Environmental Pollution* 99: 347-360.
- [63] Martin, I.T., Juniper, B.E., 1970. *The cuticles of plants*. Arnold, London.
- [64] Knoll, D., Schreiber, L., 1998. Influence of epiphytic micro-organisms on leaf wettability: wetting of the upper leaf surface of *Juglans regia* and of model surfaces in relation to colonization by micro-organisms. *New Phytologist* 140: 271 -282.
- [65] Marcell, L., Beattie, G.A., 2002. Effect of leaf surface waxes on leaf colonization by *Pantoea agglomerans* and *Clavibacter michiganensis*. *The American Phytopathological Society* 12: 1236 – 1244.
- [66] Freer-Smith, P.H., Beckett, K.P., Taylor, G., 2005, Deposition velocities to *Sorbus aria*, *Acer campestre*, *Populus deltoides* x *trichocarpa* 'Beaupre', *Pinus nigra* and x *Cupressocyparis leylandii* for coarse, fine and ultra-fine particles in the urban environment. *Environmental Pollution* 133: 157 - 167.
- [67] Grochowicz, E., Korytkowski, J., 1996. *Air protection*. Polish Educational Publisher, Ochrona Powietrza. Wydawnictwo Szkolne I Pedagogiczne 2: 17
- [68] Garland, J.A., 1983. Some recent studies of the resuspension of deposited material from soil and grass. In *Precipitation Scavenging, Dry Deposition and Resuspension* (Ed.), Pruppacher, H.R., Semonin, R.G., Slinn, W.G.N., Vol 2, pp 1087 -1097, Elsevier, Amsterdam.
- [69] Nicholson, K.W., 1993. Wind tunnel experiments on the resuspension of particulate material. *Atmospheric Environment Part A General Topics* 27: 181 - 188.
- [70] Hinds, W.C., 1986. *Aerosol Technology*. Wiley Interscience, New York.
- [71] Corn, M., Stein, F., 1965. Re-entrainment of particles from a plane surface. *American Industrial Hygiene Association Journal* 26: 325 - 336.
- [72] Muhammad, S., Wuyts, K., Samson, R., 2020. Immobilized atmospheric particulate matter on leaves of 96 urban plant species. *Environmental Science Pollution Research* 27: 36920 – 36938.
- [73] Chen, L., Liu, C., Zhang, L., Zou, R., Zhang, Z., 2017. Variation in tree species ability to capture and retain airborne fine particulate matter (PM2.5). *Nature – Scientific Reports* 1 – 11.
- [74] McIntosh, G., Gómez-Paccard, M., Osete, M.L., 2007. The magnetic properties of particles deposited on *Platanus x hispanica* leaves in Madrid, Spain, and their temporal and spatial variations. *Science of the Total Environment* 382: 135 - 146.
- [75] Postek, M.T., Vladár, A.E., 2013. Does your SEM really tell the truth? How would you know? Part I. Wiley Periodicals, Inc *Scanning* 35: 355 - 361.
- [76] Postek, M.T., Vladár, A.E., Purushotham, K.P., 2014. Does your SEM really tell the truth? How would you know? Part 2. Wiley Periodicals, Inc. *Scanning* 36: 347 -355.
- [77] Van Veld, R.D., Shaffner, T.J., 1971. Charging effects in scanning electron microscopy. *Scanning Electron Microscopy IITRI* 17 - 24.
- [78] Pawley, J.B., 1972. Charging artifacts in the scanning electron microscope. *Scanning Electron Microscopy IITRI* 153 - 160.
- [79] Shaffner, T.J., Hearle, J.W.S., 1976. Recent advances in understanding specimen charging. *Scanning Electron Microscopy IITRI* 61 - 69.
- [80] Joy, D.C., 1989. Control of charging in low voltage SEM. *Scanning* 11: 1 - 4.
- [81] Joy, D.C., Joy, C.S., 1995. Dynamic charging in low voltage SEM. *Microscopy and Microanalysis* 1: 109 - 112.
- [82] Joy, D.C., Joy, C.S., 1996. Low voltage scanning electron microscopy. *Micron* 27: 247 - 263.
- [83] Postek, M. T., Vladár, A. E., 2015. Does Your SEM Really Tell the Truth?-How Would You Know? Part 4: Charging and its Mitigation. *Proceedings of SPIE The International Society for Optical Engineering* 9636: 963605
- [84] Robinson, V.N.E., 1980. Imaging with backscattered electrons in a scanning electron microscope. *Scanning* 3: 15 - 26.